SSRG International Journal of Electrical and Electronics Engineering
ISSN: 2348-8379/ https://doi.org/10.14445/23488379/IJEEE-V13I5P108

Volume 13 Issue 5, 95-104, May 2026

Original Article

Dual-Band SIW-Based 2-Port and 4-Port MIMO Antenna for Next-Generation 5G Systems

H Vinod Kumar[1], A R Aswatha[2], Vinod B Durdi[3]

[1,3]*Department of Electronics and Telecommunication Engineering, Dayananda Sagar College of Engineering, Bangalore.*
[2]*Department of Electronics and Communication Engineering, Dayananda Sagar College of Engineering, Bangalore.*

[1]*Corresponding Author : vinod.hosakote@gmail.com*

Received: 14 February 2026 Revised: 13 March 2026 Accepted: 12 April 2026 Published: 30 May 2026

Abstract *- In this manuscript, the proposed work mainly focuses on the antenna and performance assessment of a dual-band Substrate Integrated Waveguide (SIW) Multiple-Input Multiple-Output (MIMO) antenna developed for wireless 5G systems. The new 5G communication keeps the restrictions of data speed, coverage, reliability, and capacity. Thus, antenna systems operating in the millimeter range must deliver strong performance while remaining compact and efficient. To achieve these demands, both 2-port and 4-port dual-band MIMO antenna with the SIW technique helps to improve isolation and high-power handling capacity; these configurations are proposed and analyzed. The designed antennas consist of Rogers RT/Duroid 5880 substrate and use inset-fed microstrip patch elements to operate around frequency of 28 GHz and 39 GHz. The 2-port MIMO antenna attains a gain of 7.53 dB and 5.98 dB, with impedance bandwidths of 1.53 GHz and 2.67 GHz at resonant frequencies of 28.81 GHz and 39.33 GHz. The 4-port antenna configuration performance improves further, delivering gains of 8.46 dB and 6.18 dB and bandwidths of 1.51 GHz and 2.54 GHz at 28.80 GHz and 39.46 GHz. Both MIMO antenna designs show outstanding impedance matching, with reflection coefficients below -10 dB, radiation efficiency exceeds 93%, and Voltage Standing Wave Ratio (VSWR) values within acceptable limits (VSWR ≤ 2) across the operating bands. Overall, the simulation results predict that the proposed MIMO antennas perform better and are the most suitable for high-performance next-generation 5G Technologies.*

Keywords *- Patch Antenna, MIMO, Dual-band, HFSS Tool, 5G Application*

1. Introduction

In wireless communication systems, Microstrip patch antennas have become a must-have in modern electronic systems, mainly due to their thin, small size, lightweight, and ease of fabrication [1]. Unlike traditional large metal antennas, a microstrip patch antenna is basically a flat metallic patch printed on a dielectric substrate, simple in structure, simple in design, and amazingly efficient in practice. Because of their compact arrangement feature, these antennas are mainly well-suited for limited space and portable devices. To overcome this, MIMO technology is widely used, where multiple antennas work together to improve data rate, signal quality, and reliability [2]. However, designing MIMO antennas at mmWave frequencies is not easy. Issues like mutual coupling between elements, reduced efficiency, and trouble in keeping the design compact, especially for multi-port systems, remain major challenges. To handle these difficulties, Substrate Integrated Waveguide (SIW) technology offers a practical solution [3]. It helps to improve isolation between antenna elements and minimizes losses, while keeping the structure compact and easy to fabricate. However, even after substantial progress in MIMO antenna design, numerous critical challenges remain [4]. Current antenna designs frequently suffer from one or more of the following limitations: Imperfect isolation between antenna elements, leading to higher mutual coupling.

- Trade-off between compact antenna size and high-performance gain.
- Lesser efficiency at mmWave frequencies due to substrate and fabrication limitations.
- Increased design complication when grading from 2-port to multi-port configurations.
- difficulty in attaining consistent dual-band operation with steady radiation characteristics.

In antenna design, there occurs a clear research gap in emerging a compact size, dual-band MIMO antenna system that concurrently achieves:

- High isolation
- Constant dual-band operation (28 GHz and 39 GHz).
- More gain and competence.

- Scalable multi-port configurations at 2-port and 4-port MIMO.
- Simple and practical design appropriate for real-world applications.

To link this gap, there is an essential need for an antenna design method that can sustain compactness while enhancing performance variables such as bandwidth, isolation, gain, and efficiency, mainly for mmWave 5G applications [5, 6].

The novelty of the proposed work lies in the integrated antenna design method, performance improvement, and scalability attained in a compact dual-band MIMO antenna [7]. The main novel contributions are,

- Unified SIW-based dual-port and multi-port antenna design.
- SIW Integration for enhanced isolation.
- Steady dual-band process at 28 GHz and 39 GHz.
- Compact size with high performance.
- Well-adjusted multi-port performance.

Table 1. Comparative Analysis of proposed work with recent research work on 2-port and 4-port MIMO Antenna

Ref No.	Design Area (L*W) (mm^2)	Frequency (GHz)	Gain (dBi)	Bandwidth (GHz)	Substrate	ECC	Port	DG	Efficiency %	S_{11} (dB)
[10]	5×9.7	28–38	6/8.3	2.3/6.5	Rogers RT 5880	0.00007	4	9	92/89	-21/-26
[11]	28*60	28	4.6	3.7	FR-4	0.05	2	>9.999	91	-25
[12]	23*34	39.84	3/5	8.1/13.2	FR-4	0.14	4	8.91	93	-53
[13]	8 × 7	28-38	6/7.2	1.75/6.23	Rogers RT 5880	NA	2	8.8	92/91	-36/-21
[14]	3.34 ×3.34	28-38	8/10.14	5.7-/6.7	Rogers RT 5880	0.015	4	9.92	91/93	-29/-31
[15]	27.65×12	28-38	5.2/5.3	4.2/7.1	Rogers RT 5880	0.0005	2	8.99	93/91	-30/-22
[16]	13×13	28	10	4.5	Rogers RT 5880	0.0003	4	NA	75	-25
[17]	4 × 4	28-38	10.6/ 6.65	5/5.5	FR-4	<0.0001	4	9.91	>70/ >50	-18/ -33
[18]	60 × 60	28-38	8.14/ 8.04	3.05/2.41	Rogers RT 5880	0.01	4	8.88	90/87	-21/-24
[19]	2.5×30	28-38	7.5/ 6.5	2.3/12.9	Rogers RT 5880	0.001	4	9.99	88/91	-27/ -20
[20]	0.33 × 0.33	24-38	6.32/7.21	2.45/3.52	Rogers 4350B	< 0.002	4	> 9.9	95/91	-25/-21
[21]	4.95 × 5.80	28-38	7.37/ 8.13	0.6/0.6	Rogers RO3003	0.001	4	9.9	88/88.6	-33/-21
[22]	7.5×8.8	28-38	6.6/5.86	1.06/1.23	Rogers Ro3003	0.01	2	9.8	80/85	-24/-20
Proposed	18 × 6 20×18	28-38	7.53/ 5.98	1.53/2.67	Rogers RT 5880	0.001	2 and 4	9.99	93/95	-37/-19

2. Literature Survey

Most of the existing work's emphasis is on enhancing individual performance parameters such as gain, bandwidth, and isolation, but fails to achieve a stable performance across all critical metrics [8]. The proposed antenna design efficiently addresses the following limitations by offering a balanced and optimized solution, as shown in Table 1:

- Maintains high efficiency (93 to 95%), outperforming several existing designs.
- Attains very low ECC (0.001), ensuring outstanding isolation and diversity performance
- Provides competitive gain (7.5-8.4 dBi) while keeping a compact size.
- Supports dual-band operation (28 GHz and 39 GHz) with stable performance.
- Introduces scalability from 2-port to 4-port configurations within a single structure.
- Achieves robust impedance matching (S11 as low as -37 dB), demonstrating efficient power transfer.

3. Design and Simulation of MIMO Antenna

In a wireless MIMO system, the performance is enhanced by using multiple patch elements together instead of depending on a single radiating antenna. These patches operate at the same time, allowing multiple signal paths to be transmitted and received over the same operating frequency band, rather than treating multipath effects such as reflections and scattering as a problem. MIMO systems essentially make use of them to their advantage. This approach leads to higher data rates, more reliable communication links, and more efficient use of the available spectrum, all without the need for higher transmit power. MIMO antennas are capable of supporting key techniques such as beamforming and spatial diversity. In practical terms, this means more stable connections, increased data throughput, and the ability to direct energy towards a particular region.

3.1. 2-Port MIMO Antenna Design

The design of a two-port patch antenna using the High-Frequency Structure Simulator (HFSS) tool is shown in Figure 1. The antenna consists of two identical microstrip patch radiators printed on the same dielectric substrate. The patch antenna is constructed using copper (Ground plan and Patch) and RT/Duroid 5880 (Substrate) material with relative permittivity εr = 2.2, dielectric loss tangent δ = 0.0009. The physical size of the antenna is 18 × 6 mm², and a feedline length of 1.38 mm and a width of 0.95 mm.

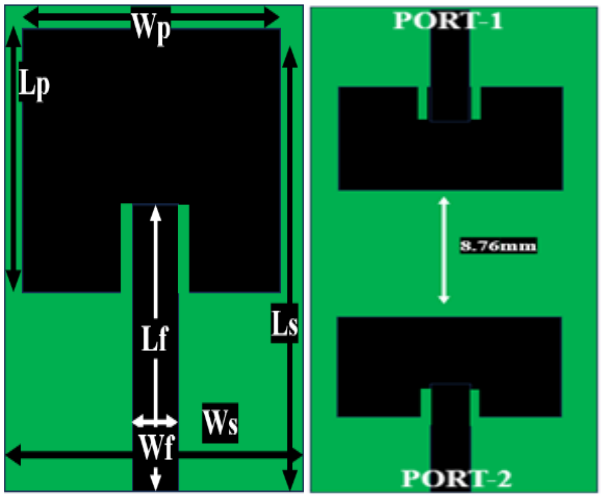

Fig. 1 Design of Rectangular antenna (a) 1-port (b) 2-port

Table 2. Antenna Parameters

Parameters	Values (mm)
Substrate/Ground Length (Ls/Lg)	6.34
Substrate/Ground Width (Ws/Wg)	7.28
Length of Patch (L_P)	0.51
Width of Patch (W_P)	3.23
Feed Width (W_f)	4.85
Feed Length (L_f)	0.95
Slot1x	3
Slot1y	1

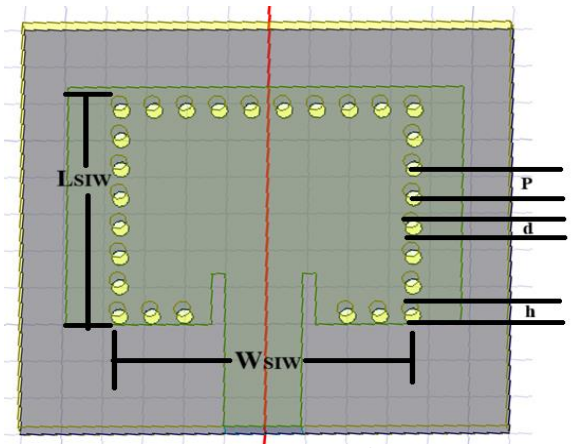

Fig. 2 The structure of SIW

The SIW design equations are,

$$\frac{P}{\lambda} < \frac{1}{10}\frac{d}{p} \geq \frac{1}{2} \quad (1)$$

$$W_{eff} = W_{SIW} - 1.08\frac{d}{p} + 0.1\frac{d^2}{W_{SIW}} \quad (2)$$

$$L_{eff} = L_{SIW} - 1.08\frac{d}{p} + 0.1\frac{d^2}{L_{SIW}} \quad (3)$$

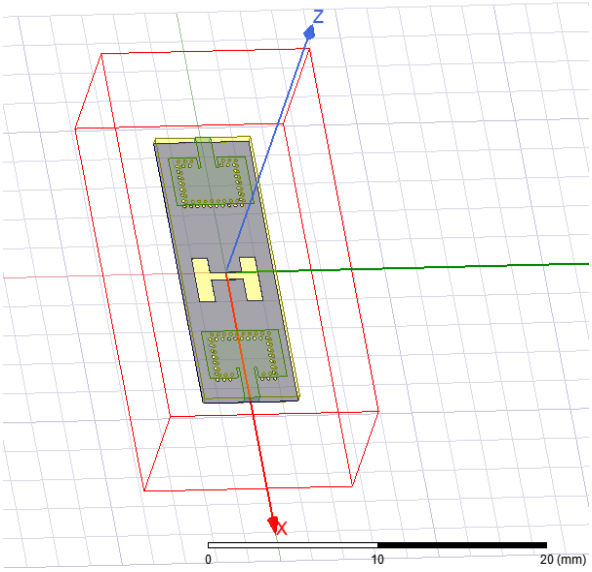

Fig. 3 Design of 2-port Microstrip patch antenna

These two patches act as Port-1 and Port-2, as shown in Figure 3, enabling MIMO operation. The patches are placed symmetrically along the length of the substrate, which helps maintain balanced radiation characteristics and consistent performance from both ports. Each Patch is excited using a microstrip feed line, and a feed network running toward the center region. The small insertion regions placed near the feed locations are used to achieve proper impedance matching,

allowing efficient power transfer from the feed line to the antenna, typically around 50 Ω. By doing this, signal reflections are kept to a minimum, which helps to maintain high efficiency and ensures that RF energy is not unnecessarily lost. The two rectangular patch elements are positioned in a way that supports spatial diversity. In real-world environments, particularly in the case of indoor environments, the communicated signals reach the reception antenna through multiple paths due to reflection, refraction, and scattering. Thus, each antenna port receives a signal with different kinds of phase variations, latency, and amplitude variations. The two patch antennas are placed apart, as they play a significant role in reducing mutual coupling.

3.2. 4-Port MIMO Antenna Design

The 4-port MIMO antenna provides a high data rate, stronger gain, and better channel capacity when compared to a 2-port MIMO antenna. The design of the projected 4-port MIMO antenna has four identical rectangular patch elements, organized in a cross-shaped manner on a single substrate and ground as shown in Figure 4. There are 4-port(feedline) attached to each antenna element, supporting more parallel data paths and improved link reliability.

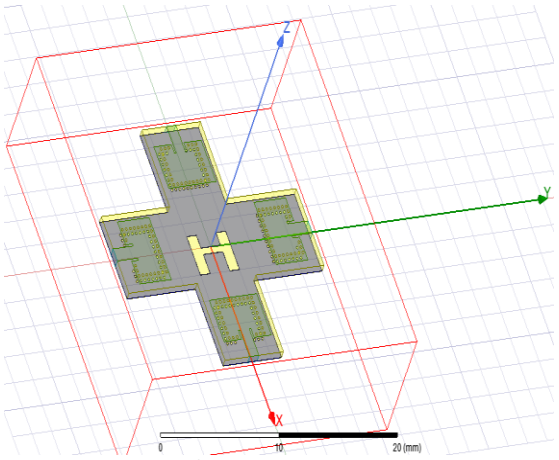

Fig. 4 Design of 4-port microstrip patch antenna

The resonant frequency of a patch antenna is commonly estimated using the transmission line model, with the overall expression given as [9]:

$$fr=\frac{c}{2L_{eff}\sqrt{\varepsilon_{eff}}} \quad (4)$$

Where 'L_{eff}' is the effective length of the Patch, 'c' represents the speed of light, and 'ε_r' denotes the effective dielectric constant.

The length extension (ΔL) can be calculated using:

$$\Delta L=\frac{0.412h(\varepsilon_{eff}+0.3)(\frac{W_p}{h}+0.264)}{(\varepsilon_{eff}-0.258)(\frac{W_p}{h}+0.8)} \quad (5)$$

The effective dielectric constant (ε_{eff}) is given by:

$$\varepsilon_{eff}=\frac{\varepsilon_r+1}{2}+\frac{\varepsilon_r-1}{2}\left(1+12\frac{h}{Wp}\right)^{-1/2} \quad (6)$$

Where, 'Wp'=Width of patch, 'h'=substrate thickness
The actual length of the Patch (L_p) can be expressed as:

$$L_p=L_{eff}-2\Delta L \quad (7)$$

The antenna width is expressed as:

$$W=\frac{c}{2fr}\times\sqrt{\frac{2}{\varepsilon_r+1}} \quad (8)$$

4. Antenna Methodology

The flow diagram of MIMO antenna design is shown in Figure 5. In which the first step is determining the operating frequency and band. This is crucial because the frequency decides almost everything: antenna size, shape, substrate choice, and even the application. The second step is antenna designing.

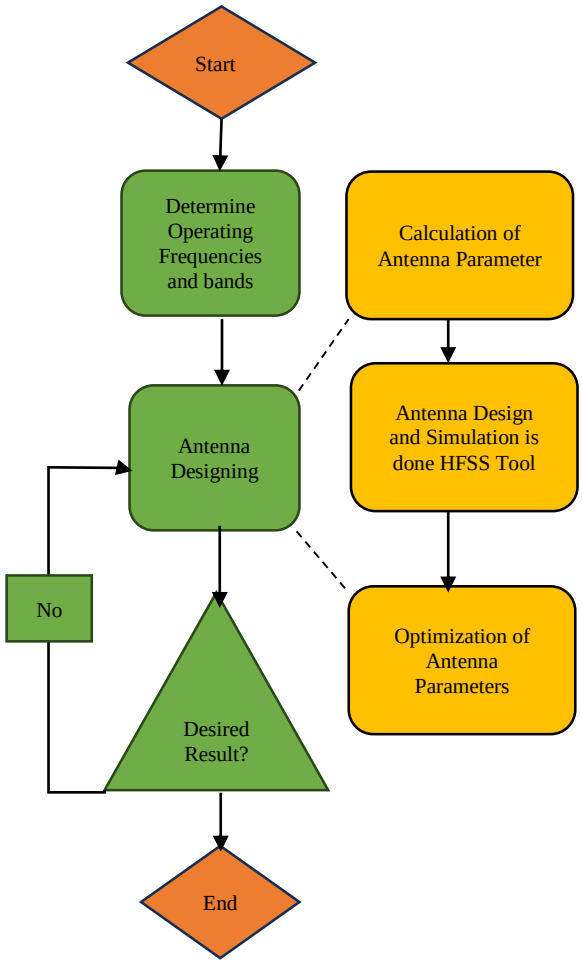

Fig. 5 Flow chart of MIMO antenna design

The design process starts by deciding the fundamental structure of the antenna, including the patch size, feeding technique, substrate properties, and the overall design. Once the reference geometry is set, the antenna design process progresses into an iterative optimization phase. The initial values of antenna parameters are obtained from analytical equations to define the preliminary values for patch/ground/substrate dimensions and feed formation. These initial values are then implemented in the HFSS simulation environment, where the antenna is modelled, and its performance is thoroughly analyzed and refined. Based on the simulation outcomes, antenna parameters are optimized. Dimensions are changed, feed positions adjusted, ground structures modified, and sometimes the whole geometry gets a small makeover. This step may be repeated several times. After optimization, if the performance does not meet the requirements, the process loops back to antenna designing and optimization. This trial-and-error cycle is continued until the simulation results are acceptable. Once the results are acceptable, indicating that the antenna meets the target frequency, bandwidth, gain, and other specifications. Thus, design is marked "Satisfied." Finally, the process reaches "End," indicating that the antenna design is complete and ready for fabrication, testing, and measurement.

5. Results and Discussions

5.1. Simulation Results of 2-port MIMO Antenna

5.1.1. Scattering Parameters

The given graph shown in Figure 6, the reflection characteristics of a 2-port MIMO microstrip antenna, represented by S11 and S22, over the frequency range of 20–50 GHz. In this context, S11 and S22 correspond to the reflection coefficient at Ports 1 and 2. These S-parameters indicate how well the antenna accepts power from the feed lines, with lower reflections meaning more efficient transfer of energy into radiation.

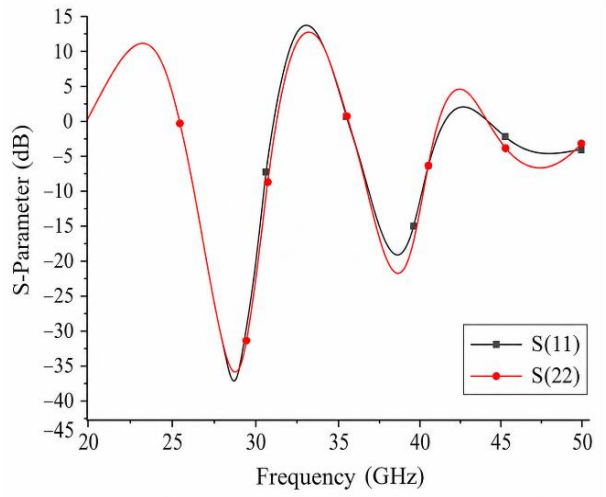

Fig. 6 The S-Parameter values of a 2-port antenna

The S11 and S22 resonates at 28.81 GHz (dip of -37.51 dB and -37.53 dB) and 39.33 GHz (dip of -18.24 dB and -19.56 dB). Such a deep dip indicates excellent impedance matching, indicating very little power is reflected, and most of the input energy is effectively radiated. Thus, the two ports maintain good impedance matching, ensuring stable and reliable MIMO performance. These values easily meet the conventional -10 dB bandwidth requirement and correspond well with the targeted 5G mmWave band.

5.1.2. VSWR

Figure 7 shows the VSWR response of the two-port MIMO antenna, with VSWR1 and VSWR2 representing the performance at Port-1 and Port-2.

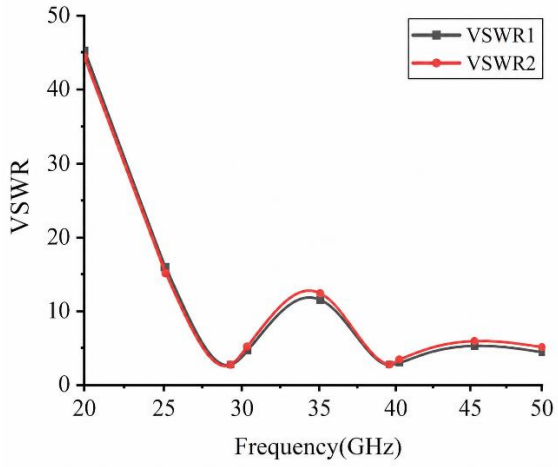

Fig. 7 The VSWR values of the 2-port antenna

As the frequency increases, the VSWR values drop sharply at two distinct point. These points clearly mark the antenna's operating frequencies, where impedance matching is strongest, and power transmission from the feedline to the Patch is most efficient:

- First operating band at 28.81 GHz
  Both VSWR1 and VSWR2 drop close to unity (1–1.1), which represents near-perfect impedance matching. At this frequency, almost all the input power is radiated with minimal reflection, confirming efficient antenna operation.
- Second operating band at 39.33 GHz
  A second VSWR minimum is observed where both ports exhibit VSWR values below 1.5, again satisfying the standard acceptance criterion of VSWR < 2. This confirms the antenna's suitability for higher mmWave communication.

5.1.3. E-Field

The given Figure 8 shows the Electric Field (E-field) distribution of the proposed 2-port MIMO microstrip antenna at its operating frequency (20 to 50 GHz). The colour distribution signifies the magnitude of the Electric Field (E-

field), the light blue region near the edge of the Patch and feedline indicates high field intensity, and blue regions indicate low field strength. From the Figure, it is observed that maximum radiation intensity appears near the edges of the antenna, indicating effective excitation of both patch elements.

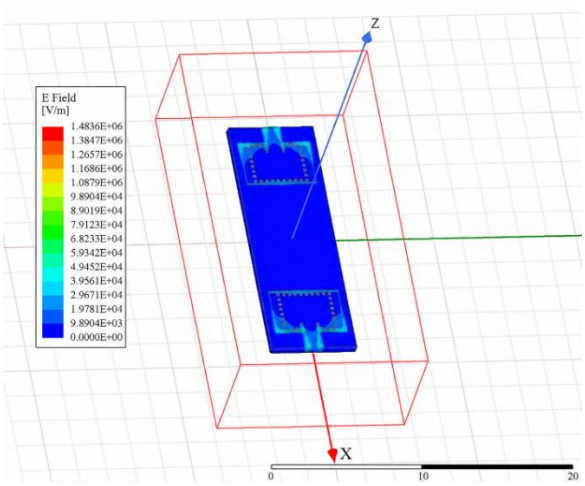

Fig. 8 The E-Field Spreading of a 2-port antenna

The distribution of the E-field is closely similar across the two radiating patch elements, which indicates:

- Both antenna ports are equally excited.
- The antenna configuration is electrically well-adjusted.
- No irregular field distribution at both antenna ports.

This similarity directly supports the observed relationship between two s-parameters (S11 and S22) and VSWR (VSWR1 and VSWR2), indicating uniform impedance matching and steady MIMO operation.

5.1.4. Directivity Gain

The graph shown in Figure 9 describes the diversity gain corresponding to each antenna port (port-1 and port-2). This performance parameter measures how MIMO antennas can fight fading and improve signal reliability. The diversity gains at both antenna ports remain consistently high, ranging from 8.8dB to 10.4 dB across the operating frequency band. This indicates that the antenna elements provide strong diversity performance over a wide bandwidth.

Two projecting peaks are observed:

- First peak around 28.81 GHz
  At this frequency, the diversity gain for both ports is around 10 dB, indicating near-ideal diversity performance.
- Second peak around 39.33 GHz
  A higher diversity gain peak (approximately 10.3–10.4 dB) is observed, confirming excellent diversity behaviour in the upper mmWave band, which is relevant for 5G systems.

Based on the diversity gain characteristics, Excellent diversity performance (DG ≈ 10 dB) is achieved near 28.81 GHz and 39.33 GHz.

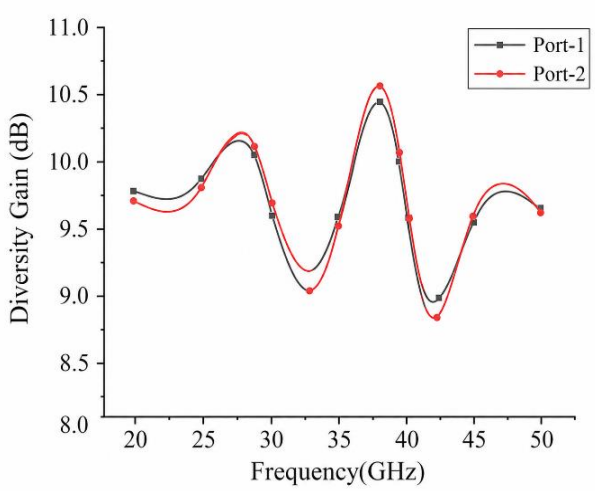

Fig. 9 The Diversity gain value of a 2-port antenna

5.1.5. Envelope Correlation Coefficient

The performance of the ECC parameter of a 2-port MIMO antenna is shown in Figure 10. The curves labelled ECC1 and ECC2 correspond to the correlation behaviour between the two antenna ports under different excitation conditions or evaluation planes.

ECC is a critical MIMO parameter that quantifies how independent the radiation patterns of the antenna elements are. Lower ECC values indicate lower correlation, which directly translates to better diversity performance, higher channel capacity, and improved link reliability.

Across the entire frequency range, both ECC1 (Port-1) and ECC2 (Port-2) remain well below 0.1, which is the commonly accepted threshold for good MIMO performance.

This confirms that the antenna maintains low mutual correlation over a wide bandwidth. Two observations that are seen in the graph below are the 2-port antenna echoes at 28.81 GHz and 39.33 GHz, and their ECC parameter approaches near-zero levels, indicating almost uncorrelated radiation paths. This confirms efficient and independent radiation from both ports in the intended operating bands.

The moderate ECC variations at intermediate frequencies are observed, with peaks remaining below approximately the value of 0.06-0.07. These fluctuations are due to frequency-dependent changes in current distribution, mutual coupling, and phase interaction between the antenna elements, since these variations do not degrade MIMO performance because ECC remains well within acceptable limits.

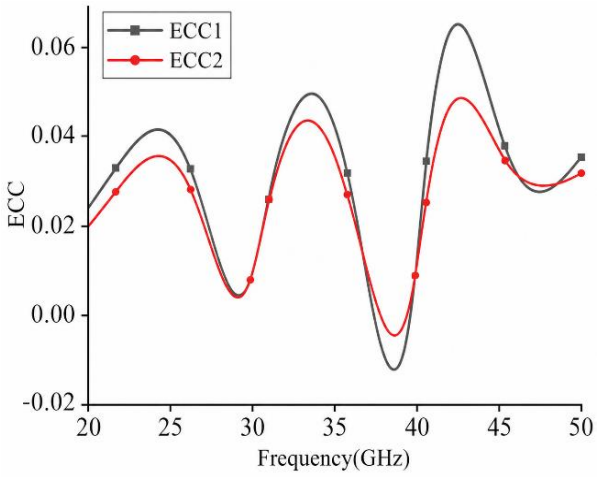

Fig. 10 The ECC values of the 2-port antenna

5.2. Simulation Results of 4-port MIMO Antenna

5.2.1. Scattering Parameters

Figure 11 shows the four-port MIMO antenna performance in terms of reflection coefficient, taken through the S-parameters S11, S22, S33, and S44. Each S-parameter curve represents the return loss seen at an individual port (1 to 4), and this helps determine whether the antenna is impedance matched or not, as well as how consistently the ports perform with respect to one another. Over the operating frequency band (20 GHz to 50 GHz), the responses of all four ports overlap, showing the same overall response. This close similarity points to a well-balanced and symmetric antenna design with uniform excitation. Maintaining such consistent performance across all ports is vital for a stable and dependable multi-port MIMO communication system.

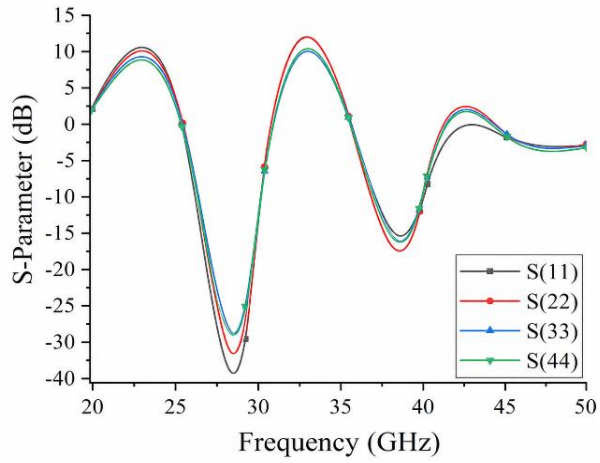

Fig. 11 The S-Parameter values of a 4-port antenna

All four ports exhibit a deep dip with S-parameter values falling well below -10 dB at two resonance frequencies (28.80 GHz and 39.46 GHz). This indicates excellent impedance matching and confirms that the antenna efficiently radiates input power successfully.

The near overlay among S11, S22, S33, and S44 specifies:

- Uniform impedance characteristics across all antenna ports.
- Negligible port imbalance.
- Good antenna fabrication tolerance and feed configuration.

This consistency is understood in a 4-port MIMO antenna to confirm stable radiation, lesser correlation, and better channel capacity.

5.2.2. VSWR

The VSWR characteristics of a 4-port MIMO antenna are shown in Figure 12. This performance parameter represents how best radio frequency power is conveyed from the transmission line to the antenna. the values of VSWR of port 1 to 4 (VSWR1, VSWR2, VSWR3 and VSWR4) further corresponds to impedance matching performance. The value of VSWR is close to one at the resonant frequency. The VSWR value close to one indicates perfect impedance matching, and the antenna works better at that frequency.

- Initially, the antenna resonates at -28.80 GHz, and all four ports have a minimum value close to unity (1.05 to 1.08). This indicates perfect antenna impedance matching. At this frequency, maximum power is transmitted from the feedline to the antenna with negligible reflection.
- Secondary operating band around -39.46 GHz, A second VSWR minimum is observed for all ports, with VSWR values remaining below 1.5, satisfying the standard acceptance criterion of VSWR<2. This confirms reliable antenna operation in the upper mmWave band.

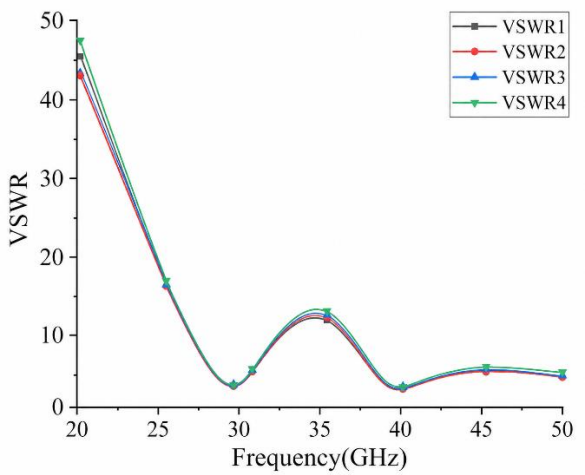

Fig. 12 The VSWR values of the 4-port antenna

5.2.3. E-Field

Figure 13 shows the E-field distribution of the proposed 4-port MIMO antenna. Similar to the E-field 2-port MIMO antenna, the intensity of the E-field is high at the edge of the radiating antenna and the feedline of the antenna.

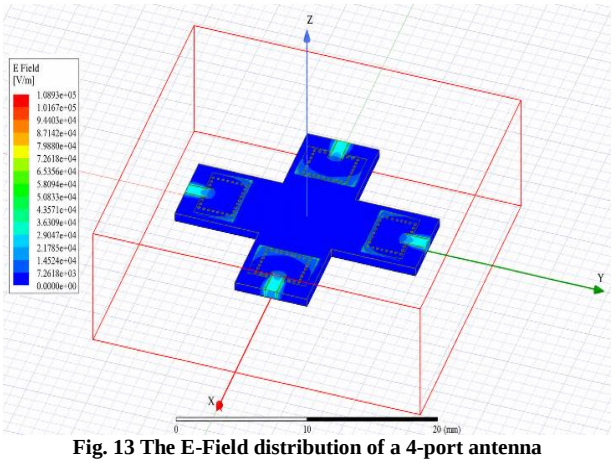

Fig. 13 The E-Field distribution of a 4-port antenna

This radiation intensity confirms that the edge radiation is typical of a microstrip patch antenna, where the fringing region at the patch margins is responsible for radiation.

5.2.4. Directivity Gain

The diversity gain of the 4-port MIMO antenna is expressed in Figure 14. The gain value of the antenna varies between 8.8 dB and 10.7 dB at 28.80 GHz and 39.46 GHz resonant frequencies. Thus, the proposed antenna has less fading and improves link reliability. This performance parameter is vital for a reliable multi-port MIMO antenna.
The near arcs of port-1 to port-4 specifies,
Balanced antenna geometry`

- Stable excitation across all ports
- Uniform radiation behaviour

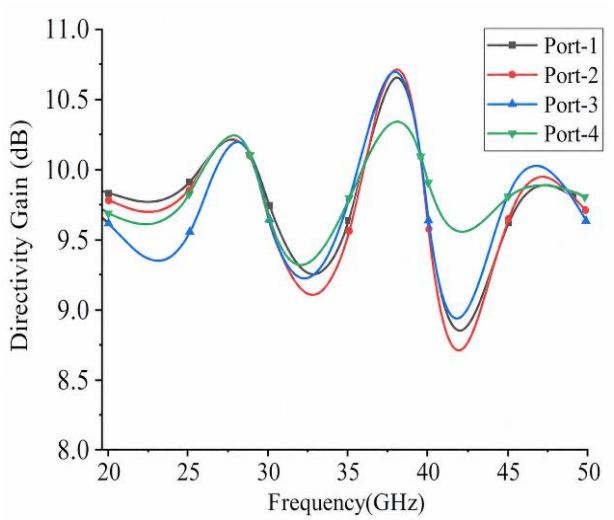

Fig. 14 The diversity gain value of a 4-port antenna

5.2.5. Envelope Correlation Coefficient

One of the key performance parameters in MIMO antennas is ECC, which describes how much one antenna component's radiation behavior overlaps with another in a MIMO system.

Lower ECC values indicate greater independence between ports, which leads to improved diversity gain, higher channel capacity, and better link reliability.

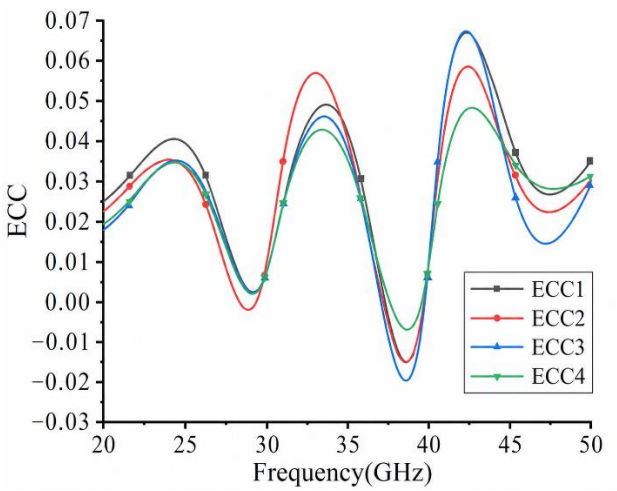

Fig. 15 The ECC values of the 4-port antenna

The performance parameter envelope correlation coefficient measures the correlation between radiation patterns and signal responses of antenna elements in an MIMO system. Lower ECC indicates antennas receive different signal paths, leading to good diversity, and high ECC antennas receive similar signals (poor diversity).

The curves shown in Figure 15 indicate ECC values at 1 to 4 ports. All the ECC curves remain well below 0.1, which is acceptable in practice. This indicates that the proposed MIMO antenna maintains low correlation among all four ports at resonating frequencies 28.80 GHz and 39.46 GHz. Overall, the ECC values approach near-zero, indicating almost uncorrelated radiation paths.

6. Conclusion

The design and simulation of proposed compact dual-band 2-port and 4-port MIMO microstrip patch antennas are best suited for 5G millimeter-wave applications at 28 GHz and 39 GHz. By using a substrate-integrated waveguide method on a Rogers Duroid 5880 substrate, the proposed antennas attained a robust balance between compact size and high performance. The simulation results of the proposed antenna show excellent impedance matching, low return loss (below -10 dB), and an acceptable VSWR (less than 1.5) value at both resonant frequencies.

It also exhibits high radiation efficiency, reliably beyond 93%, along with constant radiation characteristics and clear gain improvement. Both the MIMO antennas showed outstanding behaviour with ECC values remaining extremely low (ECC $\leq$ 0.001) and diversity gain approaching 10 dB. This provides strong isolation between antenna elements and a reliable multi-port MIMO antenna. Overall, both the proposed

2-port and 4-port MIMO antennas suggest a robust possibility for deployment in next-generation 5G systems. The design can be further extended to a massive MIMO antenna by increasing the number of antenna elements to increase channel capacity. These MIMO antennas can be used particularly for dense 5G environments and future networks. The geometry structure can be further modified and fabricated for practical integration into real-world applications like smartphones, smart watches, and wearable devices.

Conflict of Interest

The research work carried out was conducted independently and not influenced by any financial interest. The proposed work is carried out by me, and no organization is involved in it. The design and simulation of the proposed work is based exclusively based on academic and technical analysis-no funding received by any agency. Thus, there are no conflicts of interest concerning the publication of this paper.

References

[1] Shao-Hung Cheng, Shu-Chuan Chen, and Wen-Yi Huang, "Low-Profile MIMO Trapezoidal Patch Antenna for 5G Wideband Mobile Antenna Application," *IEEE Antennas and Wireless Propagation Letters*, vol. 24, no. 3, pp. 696-700, 2025. [CrossRef] [Google Scholar] [Publisher Link]

[2] Phuong Kim-Thi et al., "A Compact Design of MIMO Patch Antenna with High Gain and Symmetrical Radiation Pattern," *PLOS One*, vol. 20, no. 7, 2025. [CrossRef] [Google Scholar] [Publisher Link]

[3] Noi Truong-Quan et al., "A Method to Design Compact MIMO Patch Antenna Using Self-Isolated Technique," *Sensors*, vol. 25, no. 7, 2025. [CrossRef] [Google Scholar] [Publisher Link]

[4] Mingming Gao et al., "A 2-Port High Isolation Millimeter Wave Dual-Band Antenna Based on SIW Back-Cavity Slot," *Progress In Electromagnetics Research M*, vol. 130, pp. 29-36, 2024. [CrossRef] [Google Scholar] [Publisher Link]

[5] Siddalingappagouda Biradar, and G. S. Rajanna, "Circular Shaped 6G Wearable Patch Antennas for Wireless Body Area Network," *Body Area Networks*, vol. 666, pp. 19-30, 2026. [CrossRef] [Google Scholar] [Publisher Link]

[6] Lina Ma et al., "Bandwidth Enhancement of H-Plane MIMO Patch Antennas in Integrated Sensing and Communication Applications," *IEEE Open Journal of Antennas and Propagation*, vol. 5, no. 1, pp. 90-103, 2024. [CrossRef] [Google Scholar] [Publisher Link]

[7] Hung Tran-Huy et al., "Multi-Element Self-Decoupled MIMO Patch Antenna with Flexible Characteristics," *IEEE Access*, vol. 12, pp. 21569-21575, 2024. [CrossRef] [Google Scholar] [Publisher Link]

[8] Widad Faraj A. Mshwat et al., "Compact Reconfigurable MIMO Antenna for 5G and Wi-Fi Applications," *IEEE Access*, vol. 12, pp. 110283-110298, 2024. [CrossRef] [Google Scholar] [Publisher Link]

[9] Ketavath Kumar Naik et al., "Compact Dual-Band Four-Port MIMO Patch Antenna with Inverse U-Shaped Resonators and Defected Ground Structure for Wireless Communication Applications," *Scientific Reports*, vol. 16, pp. 1-18, 2026. [CrossRef] [Google Scholar] [Publisher Link]

[10] R. Sethumadhavi et al., "Dual and Wideband mmWave 28/38 GHz Quad Port MIMO Antenna for 5G and Beyond Applications," *Scientific Reports*, vol. 15, pp. 1-19, 2025. [CrossRef] [Google Scholar] [Publisher Link]

[11] Prem Pal Singh et al., "Development of a Dual-Port Wideband MIMO Antenna for Sub-7 GHz 5G Applications," *Scientific Reports*, vol. 15, pp. 1-25, 2025. [CrossRef] [Google Scholar] [Publisher Link]

[12] Ramesh Amugothu, Guthi Srinivas, and Siddalingappagouda Biradar, "Ultra-Compact Multiband Metasurface Absorber Enabling Advanced Healthcare Sensing Applications," *IEEE Transactions on Plasma Science*, vol. 54, no. 5, pp. 2321-2328, 2026. [CrossRef] [Google Scholar] [Publisher Link]

[13] Parveez Shariff Bhadravathi Ghouse et al., "Dual-Band Antenna at 28 and 38 GHz Using Internal Stubs and Slot Perturbations," *Technologies*, vol. 12, no. 6, 2024. [CrossRef] [Google Scholar] [Publisher Link]

[14] Md Ashraful Haque et al., "High-Isolation Dual-Band MIMO Antenna for Next-Generation 5G Wireless Networks at 28/38 GHz with Machine Learning-Based Gain Prediction," *Scientific Reports*, vol. 15, pp. 1-17, 2025. [CrossRef] [Google Scholar] [Publisher Link]

[15] Ayman R. Sabek, Wael A. E. Ali, and Ahmed A. Ibrahim, "Minimally Coupled Two-Element MIMO Antenna with Dual Band (28/38 GHz) for 5G Wireless Communications," *Journal of Infrared, Millimeter, and Terahertz Waves*, vol. 43, pp. 335-348, 2022. [CrossRef] [Google Scholar] [Publisher Link]

[16] Aditya Kumar Singh et al., "Design and Experimental Validation of a Compact Inverted l-Based Quad-Port MIMO Antenna for 5G NR mm Wave Systems," *Scientific Reports*, vol. 15, pp. 1-15, 2025. [CrossRef] [Google Scholar] [Publisher Link]

[17] Nermin Hamdan, and Çetin Kurnaz, "A Novel Dual-Band Four Port MIMO Antenna Design for 28/38 GHz Millimeter-Wave 5G Applications," *Balkan Journal of Electrical and Computer Engineering*, vol. 12, no. 4, pp. 273-281, 2025. [CrossRef] [Google Scholar] [Publisher Link]

[18] Kutay Cuneray et al., "28/38 GHz Dual-Band MIMO Antenna with Wideband and High Gain Properties for 5G Applications," *AEU - International Journal of Electronics and Communications*, vol. 162, 2023. [CrossRef] [Google Scholar] [Publisher Link]

[19] Abdulelah Alsalman et al., "Reconfigurable 28/38 GHz Wideband and High Isolation MIMO Antenna for Advanced mmWave Applications," *Journal of Electrical Engineering*, vol. 75, no. 6, pp. 467-483, 2024. [CrossRef] [Google Scholar] [Publisher Link]

[20] Moustafa M. Nasralla, "A Multi-Band Broad Bandwidth Inverted-C & F-Shaped MIMO Antenna for Enhanced Wireless Connectivity," *Results in Engineering*, vol. 28, 2025. [CrossRef] [Google Scholar] [Publisher Link]

[21] Rania R. Elsharkawy, Khalid.F. A. Hussein, and Asmaa E. Farahat, "Dual-Band (28/38 GHz) Compact MIMO Antenna System for Millimeter-Wave Applications," *Journal of Infrared, Millimeter, and Terahertz Waves*, vol. 44, pp. 1016-1037, 2023. [CrossRef] [Google Scholar] [Publisher Link]

[22] Asmaa E. Farahat, and Khalid F. A. Hussein, "Dual-Band (28/38 GHz) Wideband MIMO Antenna for 5G Mobile Applications," *IEEE Access*, vol. 10, pp. 32213-32223, 2022. [CrossRef] [Google Scholar] [Publisher Link]